

A Small Molecule Polyamine Oxidase Inhibitor Blocks Androgen-Induced Oxidative Stress and Delays Prostate Cancer Progression in the Transgenic Adenocarcinoma of the Mouse Prostate Model

Hirak S. Basu,¹ Todd A. Thompson,¹ Dawn R. Church,¹ Cynthia C. Clower,¹ Farideh Mehraein-Ghomi,¹ Corey A. Amlong,¹ Christopher T. Martin,¹ Patrick M. Woster,² Mary J. Lindstrom,¹ and George Wilding¹

¹University of Wisconsin Paul P. Carbone Comprehensive Cancer Center, Madison, Wisconsin and ²Department of Pharmaceutical Chemistry, Wayne State University, Detroit, Michigan

Abstract

High levels of reactive oxygen species (ROS) present in human prostate epithelia are an important etiologic factor in prostate cancer (CaP) occurrence, recurrence, and progression. Androgen induces ROS production in the prostate by a yet unknown mechanism. Here, to the best of our knowledge, we report for the first time that androgen induces an overexpression of spermidine/spermine N1-acetyltransferase, the rate-limiting enzyme in the polyamine oxidation pathway. As prostatic epithelia produce a large excess of polyamines, the androgen-induced polyamine oxidation that produces H₂O₂ could be a major reason for the high ROS levels in the prostate epithelia. A small molecule polyamine oxidase inhibitor N,N'-butanedienyl butanediamine (MDL 72,527 or CPC-200) effectively blocks androgen-induced ROS production in human CaP cells, as well as significantly delays CaP progression and death in animals developing spontaneous CaP. These data show that polyamine oxidation is not only a major pathway for ROS production in prostate, but inhibiting this pathway also successfully delays CaP progression. [Cancer Res 2009;69(19):7689–95]

Introduction

Advanced hormone refractory metastatic prostate cancer (CaP) is a major cause of cancer deaths among U.S. men. Most CaP patients at the time of initial diagnosis have androgen-dependent tumors that regress quickly after radical prostatectomy or radiation therapy. Unfortunately, in ~15% of the patients, the cancer recurs within a few years as an advanced hormone refractory and often-metastatic disease. Most commonly used cancer chemotherapeutic agents have little effect against advanced, metastatic CaP. Therefore, development of agents to prevent CaP occurrence, recurrence, and progression to the advanced stage is warranted.

Reactive oxygen species (ROS) such as hydrogen peroxide, superoxide, hydroxyl-free radical, and nitric oxide levels are relatively

higher in prostate epithelial cells than are in most other tissues (1, 2). Direct evidence linking ROS with an increase in tumor development in the prostate has been established (3–5). The ability of ROS to alter growth or apoptosis-related genes either by direct mutagenic effects on DNA or by alterations in gene expression and cellular signaling suggest a potential role for ROS in both initiation and progression of CaP (1–16). Oberley and colleagues (16) performed immunohistochemistry to analyze human malignant and normal prostate tissues in archival paraffin blocks. They reported that oxidative stress-induced enzymes and oxidative damage to DNA bases are relatively more abundant in malignant CaP compared with that in normal human prostate tissues. Ho and her colleagues (17, 18) used similar methods to confirm that the ROS-induced damage in spontaneously formed prostate neoplasm of transgenic adenocarcinoma of mouse prostate (TRAMP) animals are relatively more than that in normal prostatic lumen of the same animal. It has also been shown that ROS play a key role in the androgen-independent growth of androgen-dependent CaP cells (19). Therefore, understanding the biochemical pathway that modulates cellular ROS levels could yield a novel and effective therapeutic strategy to delay or even prevent CaP occurrence, recurrence, and progression. Androgen induces oxidative stress by producing ROS in normal and malignant prostatic epithelial cells (5, 10–15). The results initially published from our laboratory (10–14) have been independently confirmed by other laboratories (15, 18). Ho and colleagues (18) conclusively showed that androgen induces ROS production in rat prostatic tissues. The biochemical mechanism of androgen-induced ROS production in the prostate, however, has not yet been reported.

Our DNA microarray data from androgen-treated and untreated LNCaP human CaP cells³ suggest that androgen induces overexpression of spermidine/spermine N1-acetyltransferase (SSAT) mRNA. SSAT is the first enzyme in polyamine catabolic pathway. Polyamines are essential components of the seminal fluid. Large excess of polyamines are produced and secreted by prostatic epithelial cells and polyamine catabolism produces the ROS H₂O₂ (20–22). Thus, an induction of a rate-limiting enzyme of the polyamine catabolic pathway may be a key factor in producing a high level of ROS in the prostatic tissue.

Here, we report data from quantitative reverse transcription–PCR (qRT-PCR): lack of androgen-induced ROS production in cells

Current address for T. Thompson: University of New Mexico, College of Pharmacy, MSC 09 5360, 2502 Marble, NE, Albuquerque, NM 87131-0001; Current address for C.C. Clower: Harvard Medical School, NRB 1052, 77 Avenue Louis Pasteur, Boston, MA 02215; Current address for C.A. Amlong: University of Wisconsin School of Medicine and Public Health, Health Sciences Learning Center, 750 Highland Avenue, Madison, WI 53705; Current address for C.T. Martin: Johns Hopkins University School of Medicine, Baltimore, MD.

Requests for reprints: Hirak S. Basu, K6/522 CSC, 600 Highland Avenue, Madison, WI 53792-5669. Phone: 608-265-4912; Fax: 608-265-8133; E-mail: hsb@medicine.wisc.edu.

©2009 American Association for Cancer Research.
doi:10.1158/0008-5472.CAN-08-2472

³ Thompson et al., manuscript in preparation.

transfected with small interfering RNA (siRNA) against SSAT, SSAT enzyme activity, and cellular polyamine levels in LNCaP cells. These data confirm that androgen induces both SSAT expression and enzyme activity in androgen-treated LNCaP human CaP cells. A small molecule inhibitor of N1-acetyl polyamine oxidase (APAO) *N,N'*-butanedienyl butanediamine (MDL 72,527 or CPC-200; refs. 23, 24) completely blocks androgen-induced ROS production in LNCaP cells, as well as in the prostatic lumen of the TRAMP animals. CPC-200 treatment also inhibited tumor growth and significantly increased the life expectancy of TRAMP animals. These data clearly show that polyamine oxidation is the major biochemical pathway for generating oxidative stress in the prostatic epithelial cells. Blocking polyamine oxidation is a valid strategy for lowering oxidative stress in the prostate and prevents CaP progression, showing a direct link between prostatic ROS and CaP progression.

Materials and Methods

Materials

CPC-200 has been synthesized by Prof. Patrick Woster following a previously published procedure (23). The LNCaP human prostate carcinoma cell line was purchased from the American Type Culture Collection. All enzymes and assay kits were purchased from manufacturers described in the Methods (see below).

Methods

Tissue culture. Cells were maintained in DMEM supplemented with 5% fetal bovine serum, nonessential amino acids, and 1% streptomycin-penicillin in a humidified 95% air/5% CO₂ atmosphere. Cells were harvested by treatment for 3 to 5 min with STV (saline A, 0.05% trypsin, 0.02% EDTA) at 37°C following a previously published procedure (12).

Androgen deprivation. Cells collected for experiments were counted and cultured in medium containing 4% charcoal-stripped serum plus 1% nonstripped serum (F1/C4) for 48 h. This combination of stripped and nonstripped serum was previously shown to sufficiently deplete androgen content while limiting adverse growth effects not related to hormone depletion that occur with the use of 5% stripped serum (12). Concurrently in each experiment, cells were seeded in 96-well tissue culture plates at a density of 2,500 cells per well in 100 µL medium for the measurement of ROS as an indicator of redox status. DNA levels were measured as an indicator of growth (see below). LNCaP cells were seeded in F1/C4 at a density of 1×10^6 cells per 10-cm tissue culture plate for protein estimation for Western blot analysis (see below). Protein estimation was carried out following standard procedure previously published from our laboratory (10).

qRT-PCR. Total RNA from LNCaP cultures was isolated using the RNeasy kit (Qiagen) according to the manufacturer-supplied protocol. For qRT-PCR analysis, cDNA was produced from total RNA using Superscript (Invitrogen), according to the manufacturer's instructions. qRT-PCR was performed using the iQ SYBR Green Supermix (Bio-Rad Laboratories, Inc.), according to the manufacturer's instructions, with thermal cycling parameters of 1 cycle of 95°C for 10 min followed by 40 cycles of a 96°C denaturation for 15 s and a 60°C annealing/extension for 1 min using an iCycler (Bio-Rad), following a published procedure (10). To control for variability in efficiency of cDNA synthesis between samples, cDNA levels of the genes under investigation were normalized to the cDNA levels of glyceraldehyde-3-phosphate dehydrogenase (GAPDH). PCR primer sequences were designed using Oligo 5.0 software (National Biosciences) and synthesized at the University of Wisconsin Biotechnology Center. The PCR primer set sequences were as follows: GAPDH forward primer, AAA TTC CAT GGC ACC GTC AA and reverse primer, TCT CGC TCC TGG AAG ATG GT; SSAT forward primer, CGA GCT CGA GAG GGG CCT GGT CCG CAA A and reverse primer, GTT CGA ATT CTA AAG CTT TGG AAT GGG TGC TCA.

siRNA transfection and isolation of stable LNCaP clone siSSAT.

Construction of pSIF-H1-siSSAT vector. Stable expression of siRNA for SSAT was used to suppress SSAT expression in LNCaP cells. Oligonucleo-

tides for silencing SSAT were designed based on the published sequence (25). The oligonucleotides were synthesized by Invitrogen. The annealed oligonucleotides were inserted into pSFI1 vector (SBI; System Biosciences).

Transduction of LNCaP cells by pPACKaged pSIF-H1-siSSAT or pSIF-H1-siLuc. LNCaP cells stably expressing pSIF-H1-siSSAT vector were established using lentiviral system from SBI, following the manufacturer's instructions. Briefly, the day before transfection, 5×10^6 293NT cells were seeded in a 10-cm plate in complete medium without antibiotics. The following day, 2 µg expression vector pSIF-H1 carrying siSSAT or vector control (pSIF-H1-siLuc) were separately mixed with 10 µg pPACK (Packaging Plasmid Mix; SBI) and 30 µL of Lipofectamine (Invitrogen) in medium without serum and antibiotics. The mixture was added to 293NT cells in 2% serum without antibiotics. After overnight incubation at 37°C in a 5% CO₂ incubator, the medium was replaced with fresh 2% serum containing antibiotics, and the incubation was continued for another 48 h at 37°C in a 5% CO₂ incubator. The supernatant was harvested by centrifugation at 5,000 rpm for 5 min and used for transducing 1×10^5 LNCaP cells, which were plated in polylysine plate (BD Bioscience) the day before transduction. Puromycin (Sigma; 1 µg/mL) in complete medium was used for selection of stably transduced cells for pSIF-H1-si SSAT and vector control. The silencing of SSAT in these cells was verified by qRT-PCR (see below).

Reduced 2',7'-dichlorofluorescein diacetate oxidation assay. The 96-well culture plates were assayed for estimation of ROS levels in intact cells using the fluorescent dye 2',7'-dichlorofluorescein diacetate (DCF; Molecular Probes, Inc.) following a published procedure (12). In brief, cell cultures were washed with 200 µL Krebs' Ringer buffer prewarmed to 37°C, incubated as usual at 37°C in 100 µL Krebs' Ringer buffer containing 10 µg/mL (final concentration) DCF dye for 45 min. Each 96-well culture plate was scanned on a CytoFluor 2350 plate scanner (Applied Biosystems) using the 485/530 nm filter excitation and emission set and then frozen at -70°C for the subsequent analysis of DNA content.

DNA assay. For DNA analysis, each culture plate frozen to -70°C was thawed/equilibrated to room temperature in the dark. Hoechst dye was then added to each well in 200 µL of high salt TNE buffer [10 mmol/L Tris, 1 mmol/L EDTA, 2 mol/L NaCl (pH 7.4)] following a published procedure (12). After further incubation at room temperature for over 2 h under protection from light, culture plates were scanned on a CytoFluor 2350 scanner using the 360/460 nm filter excitation and emission set. The DCF fluorescence units were normalized to the Hoechst-DNA fluorescence units for each well and used as a measure of the level of ROS being generated. The DNA fluorescence units were also used as a measure of cell growth.

SSAT assay. SSAT assay was performed following essentially the same procedure published elsewhere (26). Cells in monolayer were washed twice with PBS and resuspended in 5 mmol/L HEPES buffer (pH 7.2) containing 1 mmol/L DTT. Cells were lysed by three 30-s pulses of sonication. Cell lysates were centrifuged, and cytoplasmic contents were collected and stored at -80°C. On the day of the assay, the cytoplasmic contents were incubated with 150 pmol of spermidine and 500 pmol of ¹⁴C-acetyl CoA (GE Healthcare/Amersham) in 25 µL HEPES buffer for 30 min. The reaction was stopped by cooling in ice and by an addition of chilled 10 µL of hydroxylamine hydrochloride and then heating in a boiling water bath. After centrifugation, the supernatant was spotted on a phosphocellulose filter, washed, and counted. Cytosolic protein contents were determined by Bradford method, and the results are expressed as picomoles of acetyl spermidine synthesized per minute per milligram protein.

Polyamine analysis. A known number of cells ($>1 \times 10^6$) were taken from harvested samples and centrifuged at $800 \times g$ at 4°C for 5 min. The cells were washed twice with chilled Dulbecco's isotonic phosphate buffer (pH 7.4) by centrifugation at 1,000 rpm at 4°C and resuspended in the same buffer. After the final centrifugation, the supernatant was decanted and 250 µL of 8% sulfosalicylic acid were added to the cell pellet. The cells were sonicated, and the mixture was kept at 4°C for at least 1 h. After further centrifugation at $8,000 \times g$ for 5 min, the supernatant was removed for analysis following a published high-performance liquid chromatography (HPLC) procedure (27). Because polyamine levels vary with environmental conditions, control cultures were sampled for each experiment.

Animals. TRAMP mice were a kind gift from Dr. Norman Greenberg, and a new colony has been established and maintained at the University of Wisconsin. FVB mice were obtained from Harlan Sprague-Dawley and bred with TRAMP females to produce TRAMP × FVB[F1] mice for these studies. Male TRAMP × FVB mice were confirmed positive for the TRAMP transgene by PCR following published protocols (28). Animal care and use were in accordance with protocols approved by the University of Wisconsin-Madison School of Medicine and Public Health Animal Care and Use Committee and the NIH Guide for the Care and Use of Laboratory Animals.

Results

Androgen induces SSAT mRNA expression. LNCaP cells cultured in androgen-depleted medium (see Materials and Methods) were treated for 96 hours with 0.05 and 1 nmol/L of the androgen analogue R1881. Results published from our laboratory have shown that 1 nmol/L R1881, which closely resembles the androgen levels in normal male human serum, produces high ROS levels in LNCaP cells after a 96-hour treatment, whereas 0.05 nmol/L R1881 causes a minor decrease in cellular ROS (10–14). We have performed qRT-PCR experiment to detect the expression of SSAT mRNA in cells treated with 0, 0.05, and 1.0 nmol/L R1881. The expression of GAPDH mRNA has been used as a control to normalize the qRT-PCR data. The results for the 96-hour treatment are shown in Fig. 1A. qRT-PCR data show that ~25-fold to 30-fold increase in the SSAT mRNA level only in 1.0 nmol/L R1881-treated cells and not in untreated or 0.05 nmol/L R1881-treated cells. The time course of SSAT mRNA production after treatment with 1 nmol/L R1881 is shown in Fig. 1B. The induction of SSAT mRNA production has not been observed up to 48 hours and has been observed only between 48 and 72 hours of androgen exposure. The ROS levels of LNCaP cells treated with varying concentrations of R1881 for different times are shown in Fig. 1C. The ROS levels do not increase for 48 hours after treatment and start increasing only between 48- and 72-hour treatment. Thus, these data show that the androgen-induced SSAT gene expression that causes polyamine oxidation and ROS production runs parallel to the time course of androgen-induced ROS production in LNCaP cells. It is also evident that SSAT gene expression is induced only at androgen concentration that increases ROS but not at androgen concentration that does not increase cellular ROS.

Androgen-induced changes in cellular polyamine level confirm an increase in SSAT enzyme activity. To test if the increase in SSAT mRNA level also translates into higher SSAT enzyme activity, we have tested the effect of androgen on cellular polyamine and acetyl polyamine (Ac-polyamine) levels in untreated LNCaP cells and cells treated with 1 nmol/L R1881 for 96 hours. We have also pretreated the cells with 25 μ mol/L APAO inhibitor CPC-200 to test the efficacy in inhibiting APAO as observed by the effect on androgen-induced changes in cellular polyamine levels. Under our culture conditions, it has been reported that 25 μ mol/L CPC-200 completely inhibits APAO in most cell lines, including CaP cells (23, 24). The polyamine and Ac-polyamine levels in cells treated with 0 and 1 nmol/L R1881 for 96 h with or without 24 h pretreatment with 25 μ mol/L CPC-200 are shown in Fig. 2. R1881 (1 nmol/L) treatment for 96 hours increases putrescine and spermidine levels by 6-fold to 10-fold, decreases spermine levels by one-half, and markedly increases *N*-acetyl spermidine and *N*-acetyl spermine levels that are undetectable in untreated cells. These results confirm that androgen treatment not only increases the SSAT mRNA level (Fig. 1) but also enhances SSAT enzyme

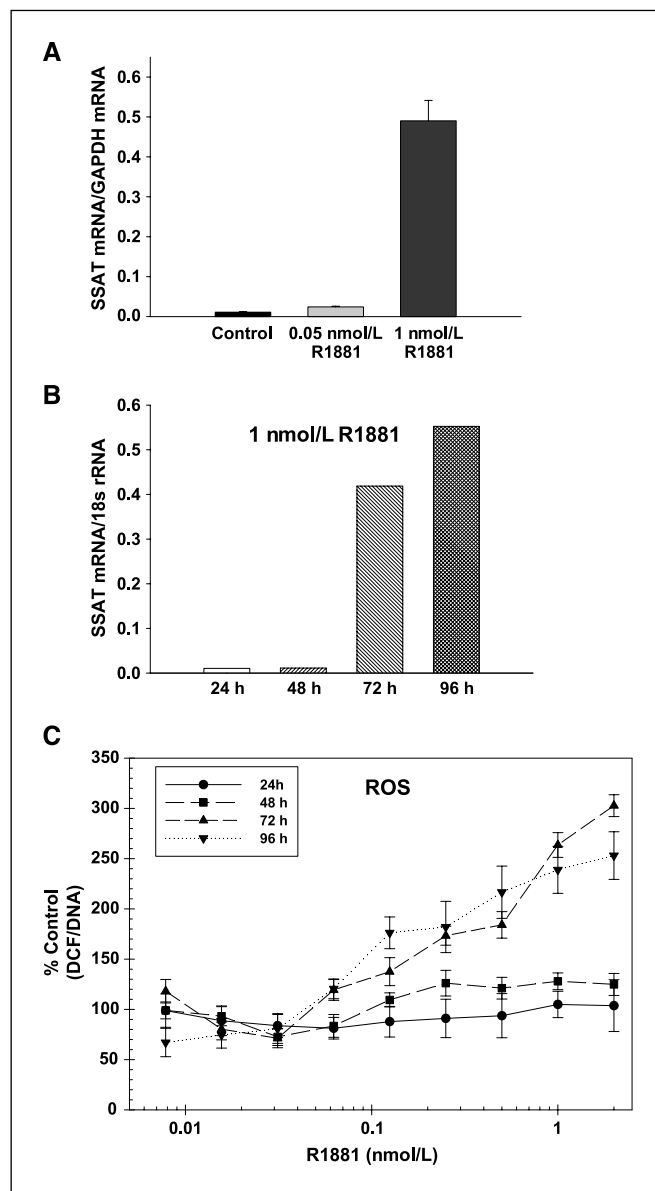


Figure 1. qRT-PCR amplification of SSAT mRNA from LNCaP cells: A, either control untreated (■) or treated with 0.05 nmol/L (□) and 1 nmol/L R1881 (▨) for 96 h; B, treated with 1 nmol/L R1881 for 24 h (□), 48 h (▨), 72 h (▩), and 96 h (▧); C, ROS levels in LNCaP cells determined by DCF assay (see text) after treatment with graded concentrations of R1881 at 24 h (●), 48 h (■), 72 h (▲), and 96 h (▼) after treatment. All mRNA data are normalized to corresponding GAPDH mRNA expression. All ROS data are normalized to corresponding LNCaP cells grown in the absence of androgen (F1/C4 medium). The data are average of readings from six identically treated wells repeated twice in triplicates, and error bars represent the exponent of the variance of data distribution.

activity, which causes the increase in spermidine and spermine catabolites—Ac-polyamines, putrescine, and spermidine. CPC-200 treatment alone has little effect on most cellular polyamine levels (except for a small increase in acetyl spermine level). In 1 nmol/L R1881-treated cells, however, CPC-200 pretreatment almost completely blocks the R1881-induced increase in putrescine and spermidine levels and causes 3–4-fold increase in *N*-acetyl-spermidine and *N*-acetyl-spermine levels without appreciably changing spermine level. These data, in addition to a small but significant increase in *N*-acetyl-spermine level in cells treated only

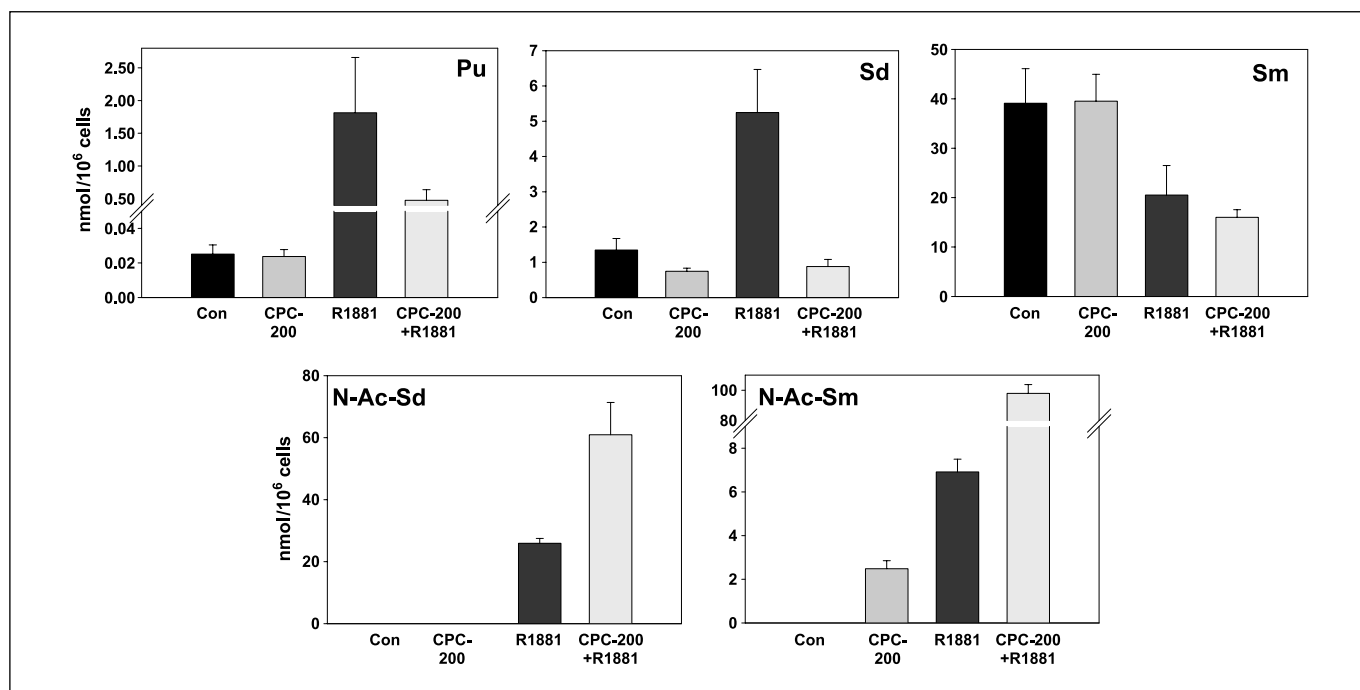


Figure 2. Putrescine (*Pu*), spermidine (*Sd*), spermine (*Sm*), *N*-acetyl spermidine (*N-Ac-Sd*), and *N*-acetyl spermine (*N-Ac-Sm*) levels of LNCaP cells treated as follows: control (■), 25 μmol/L CPC-200 for 120 h (▒), 1 nmol/L R1881 for 96 h (■), 25 μmol/L CPC-200 for 24 h followed by 1 nmol/L R1881 for 96 h (▒). All data points and SDs are calculated from the results of two separate experiments run in triplicates.

with CPC-200, show that 25 μmol/L CPC-200 efficiently blocks APAO enzyme activity, thus inhibiting polyamine oxidation and increasing cellular *N*-acetyl-polyamine levels. In addition, the increase in Ac-polyamines also shows that CPC-200 alone has little effect on the SSAT gene expression and/or SSAT enzymatic activity in the androgen-treated cells.

Androgen-induced ROS production is relatively lower in SSAT siRNA transfected LNCaP cells. To further confirm that SSAT is the major player in androgen-induced ROS production in LNCaP cells, we have constructed one LNCaP cell clone stably transfected with siRNA against SSAT (siSSAT). The ability of the siRNA to reduce SSAT mRNA level was first confirmed using qRT-PCR. The results are shown in Fig. 3A. These data have been normalized to the 18S rRNA level. The results show that 1 nmol/L R1881-induced increase in SSAT mRNA level in the siSSAT clone is nearly 80% less than that observed for 1 nmol/L R1881-treated LNCaP cells transfected with a control vector. The acetylated polyamine levels in the vector control and siSSAT-transfected cells are shown in Table 1. Cells expressing siSSAT show over 4.5-fold decrease in acetylated spermidine and over 30-fold decrease in acetylated spermine level, which confirms that the decrease in mRNA level parallels a decrease in SSAT enzyme activity. The SSAT enzyme activity in R1881-treated and untreated LNCaP cells, cells transfected with a control vector, and siSSAT-transfected cells are shown in Fig. 3B. In both wild-type LNCaP cells and cells transfected with a control vector, the SSAT enzyme activity has been increased by over 2-fold. In siSSAT transfected cells, however, the enzyme activity is less than half of the other two cell lines and the activity does not change after R1881 treatment. The effects of 1 nmol/L R1881 treatment on the ROS levels in LNCaP cells and siSSAT clone as determined by a DCF dye oxidation assay are shown in Fig. 3C. R1881 treatment has no significant effect on ROS

production in siSSAT clone compared with a nearly 1.5-fold increase induced by R1881 in LNCaP cells transfected with the control vector. The difference in percentage induction of ROS levels in wild-type versus siSSAT clone is statistically significant with a *P* value of <0.001 as determined using a two-tailed Student's *t* test.

CPC-200 treatment completely blocks androgen-induced ROS production in LNCaP cells. To test if CPC-200 treatment can also block the androgen-induced ROS production in the wild-type LNCaP cells, we have determined the relative changes in ROS levels in LNCaP cells that are either untreated or pretreated for 24 h with 25 μmol/L CPC-200 and exposed to graded concentrations of R1881 for 96 h. The results of ROS measurement in CPC-200 pretreated and untreated cells exposed to increasing androgen concentrations are shown in Fig. 4. Data points, SDs, and *P* values are calculated from the reading of six wells of a 96-well plate, wherein each plate was run in triplicate and the experiment was repeated twice. CPC-200 (25 μmol/L) pretreatment not only completely blocks the R1881-induced ROS production, the ROS levels of CPC-200 pretreated cells are actually even lower than that of control androgen-untreated cells. These data confirm that polyamine catabolism is one of the major causes of the ROS production of prostate cells in general and androgen-induced enhancement of ROS in androgen-dependent CaP cells in particular.

We have not observed any effect of CPC-200 pretreatment on the androgen receptor level in both androgen-treated and untreated cells (data not shown), indicating that the decrease in cellular ROS is not due to changes in cellular androgen receptor level in CPC-200-treated cells.

CPC-200 treatment markedly reduces tumor formation in TRAMP animals and significantly increases life expectancy. To determine if CPC-200 treatment induced reduction in the ROS levels and delays prostate tumor progression *in vivo*, we tested

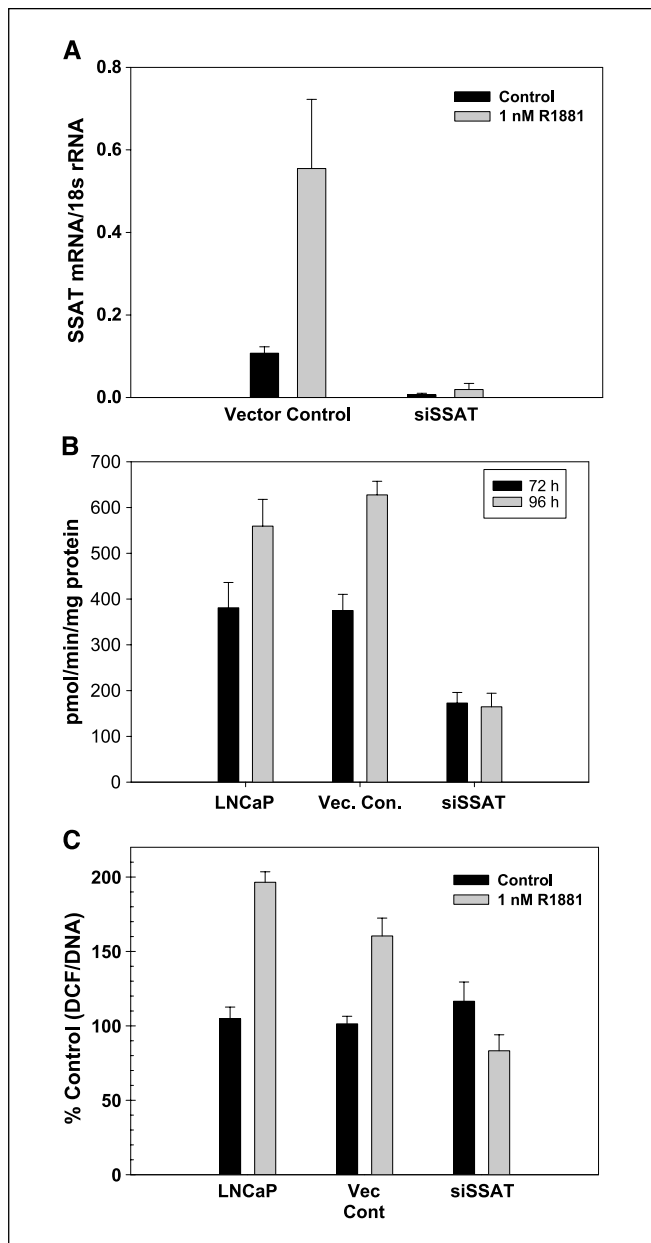


Figure 3. A, qRT-PCR amplification of SSAT mRNA from LNCaP cells stably transfected with siSSAT vector and scrambled vector control (see Materials and Methods for detail). Cells are either grown in the presence of 0 nmol/L (■) or 1 nmol/L R1881 (□). All data are normalized to corresponding 18S rRNA expression. The data are average of readings from six identically treated wells repeated twice in triplicates, and error bars represent the exponent of the variance of data distribution. B, SSAT enzyme activity in picomoles of acetyl spermidine formed per milligram protein per minute in wild-type LNCaP cells, LNCaP cells transfected with control vector, and LNCaP cells transfected with siSSAT either vehicle treated (■) or treated with 1 nmol/L R1881 for 96 h (□). Each data point and SDs are calculated from cell extracts from three independent experiments, and each extract is run in two separate assays that are run in triplicates. C, cellular ROS levels as determined by the DCF assay (see text) for LNCaP cells stably transfected with vector control and siSSAT either untreated (■) or treated with 1 nmol/L R1881 (□). All data were normalized to the ROS level of untreated control LNCaP cells grown in the absence of androgen (F1/C4 medium). Data points and SDs were calculated from the results of two separate experiments, each run in triplicate 96-well plates.

its effect on tumor formation in TRAMP × FVB hybrid animals (29) that spontaneously develop palpable prostate tumors by ~ 12 to 16 weeks of age, and all die due to CaP. We tested a dose of 25 mg/kg of CPC-200 given i.p. biweekly over a period of 10 weeks for a total

Table 1. Acetylated polyamine levels (nmol/10⁶ cells) in vector control and siSSAT clones of LNCaP cells

	Vector control		siSSAT	
	N-Ac-Sd	N-Ac-Sm	N-Ac-Sd	N-Ac-Sm
Control untreated	NQ	ND	NQ	ND
1 nmol/L R1881	33.3 ± 6.9	6.3 ± 2.6	7.2 ± 2.5	0.21 ± 0.15

NOTE: Acetylated spermidine and spermine levels in untreated and R1881-treated LNCaP cells transfected with either control vector or vector expressing siSSAT. Mean ± SDs of two separate experiments run in triplicates. All data are in nmol/10⁶ cells. Abbreviations: N-Ac-Sd, N-acetyl spermidine; N-Ac-Sm, N-acetyl spermine; NQ, not quantifiable; ND, not detectable.

of six treatments. This dose is slightly above the 20 mg/kg dose required to completely inhibit mouse APAO enzyme activity *in vivo* and is well below the maximum tolerated dose of CPC-200 in mice (100 mg/kg daily for 14 days; ref. 24). This dose has shown no overt toxicity and no observable side effects in mice. In our study, no overt sign of toxicity, abnormal behavior, body weight loss, or any other observable symptom was detectable, either short term after each of the successive CPC-200 injections or long term until the end of the study.

The difference in median survival time was assessed using a Wilcoxon rank sum test. Across two independent studies that include a total of 26 animals per arm, we have observed median survival of 12.0 weeks versus 17.5 weeks after first treatment for vehicle control versus CPC-200-treated mice, yielding a statistically significant ($P = 0.03$) improvement in median survival by 5.5 weeks for CPC-200-treated animals (Fig. 5). As treatment has begun at an average age of 8 weeks in these studies, this equates to median survival ages of ~20 weeks for control and ~25 weeks for CPC-200-treated animals. Therefore, six injections of CPC-200 have resulted in >25% increase in overall life expectancy.

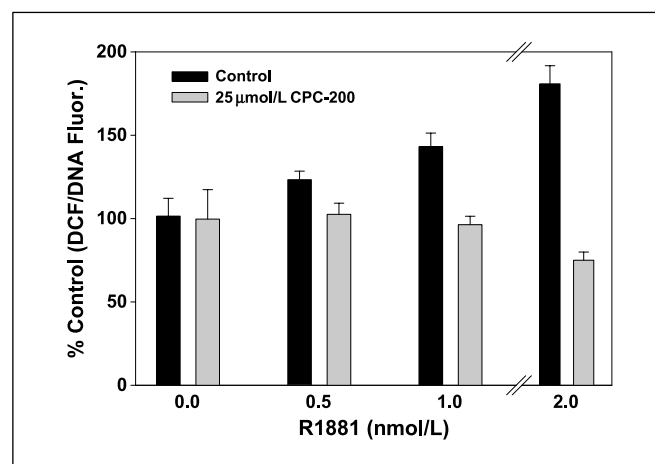


Figure 4. ROS levels in cells treated with graded R1881 concentration that are either vehicle treated (■) or treated with 25 μmol/L CPC-200 (□). All data are normalized to the ROS level of untreated control LNCaP cells grown in the absence of androgen (F1/C4 medium). Data points and SDs are calculated from the results of two separate experiments, each run in triplicate 96-well plates.

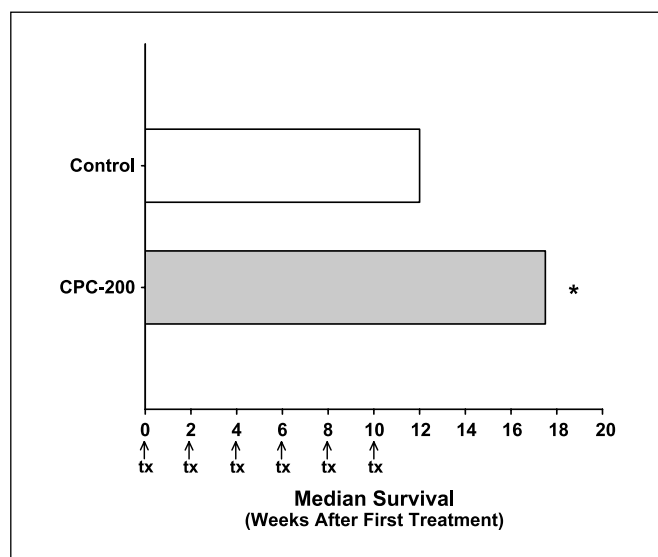


Figure 5. Median survival of TRAMP \times FVB mice treated with CPC-200 compared with vehicle control. TRAMP \times FVB[F1] male mice are treated with 25 mg/kg CPC-200 (■) or saline vehicle control (□) i.p. once every 2 wk from week 0 through week 10 for six treatments total beginning at an average age of 8 wk. Difference in median survival time was assessed using the Wilcoxon sum rank test (two studies were performed for a total 26 animals each in treated and untreated arms). *, $P = 0.03$.

Discussion

The data presented here conclusively show that androgen-induced activation of SSAT, the first enzyme of one major polyamine oxidation pathway, is a key source of oxidative stress in the prostatic lumen and is one of the major factors in prostate tumor progression. The data establish that CPC-200, a small molecule specific inhibitor of polyamine oxidase, cannot only block androgen-induced oxidative stress in cultured LNCaP human CaP cells but can also significantly delay prostate carcinogenesis in TRAMP \times FVB animals. These results open up a new avenue for research in CaP therapy.

The fold increase of SSAT mRNA level estimated using qRT-PCR in siSSAT clone is nearly 80% less than that observed for wild-type LNCaP cells (Fig. 3A). This decrease in SSAT mRNA level is sufficient to completely block androgen-induced ROS (Fig. 3B). Casero and colleagues (21, 22) have reported the detection, isolation, and characterization of another inducible polyamine oxidase (PAOh1) in human breast, colon, lung, and prostate tumors. PAOh1 oxidizes unacetylated polyamines and also produces H_2O_2 . PAOh1-induced ROS production, however, does not go through APAO pathway and has been reported to be the primary source of ROS in breast cancer cells and not specific for CaP metabolism. Almost complete block of androgen-induced ROS production in SSAT mRNA silenced cells (Fig. 3B) suggests that PAOh1 probably plays a minor role in the androgen-induced ROS production specifically in the CaP cells.

The ability of CPC-200 treatment to reduce cellular ROS production (Fig. 4) also shows that an overexpression of SSAT that initiates enhanced polyamine catabolism is one of the major causes of androgen-induced oxidative stress in androgen-dependent human CaP cells. Because the enzyme PAOh1 is also inhibited by CPC-200 (21, 22), some contribution of PAOh1 activity in the cellular oxidative stress cannot be completely ruled out. It is to be noted, however, that androgen treatment decreases cellular spermine levels and increases cellular acetyl-polyamine level (Fig. 2). The

polyamine levels in R1881 (Fig. 2) and the reduction of ROS levels in cells treated with 25 μ mol/L CPC-200 (Fig. 4) suggest that most of the ROS production in R1881-treated cells is due to SSAT induction followed by oxidation of acetylated polyamines by constitutively expressed APAO rather than a direct oxidation of spermine by PAOh1.

It is also to be noted that CPC-200 pretreated LNCaP cells growing in the presence of 1 nmol/L R1881 have even less ROS than do untreated cells (Fig. 4). This suggests that the basal level of ROS produced in LNCaP cells growing in the absence of androgen may also be due to low grade oxidation of cellular polyamines that is now blocked by CPC-200 treatment.

As spermine acts as a scavenger for ROS (30), androgen-induced decrease in polyamine levels may also cause the observed increase in ROS levels. CPC-200 (25 μ mol/L) pretreatment, however, does not reverse androgen-induced reduction of cellular spermine levels (Fig. 2), although it completely blocks the ROS production (Fig. 4). Therefore, R1881 induced depletion of the cellular spermine level can be ruled out as a major contributor to the increase in the ROS levels.

Our Western analysis for androgen receptor protein expression showed no effect of CPC-200 treatment on androgen receptor levels (data not shown). Thus, we rule out the possibility of CPC-200-induced changes in androgen receptor expression as a cause for the changes in growth and/or ROS.

We have established preclinical efficacy of CPC-200 using the TRAMP \times FVB mouse model of prostate carcinogenesis. CPC-200 at a well-tolerated dose of 25 mg/kg given i.p. once every 2 weeks for a total of six treatments significantly inhibited the growth of tumors in this model as evidenced by improved survival (Fig. 5). In our studies, the majority of mice (>90%) were sacrificed due to reaching a predefined tumor size per our animal protocol, thus survival is a surrogate for tumor burden and improvement in survival thus equates with an inhibition of tumor growth by CPC-200 in our TRAMP \times FVB model. Therefore, the significant 5.5-week improvement ($P = 0.03$) in median survival for CPC-200 using this model (Fig. 5) shows the ability of CPC-200 to slow prostate tumor growth. The efficacy of CPC-200 against prostate tumor progression in this animal model supports the hypothesis that polyamine oxidation and resultant increase in ROS play an important role in prostate carcinogenesis and strongly implicates the potential of CPC-200 as a new therapeutic agent for CaP.

Several mechanisms such as expression (or nuclear translocation) of specific transcription factors, such as hypoxia-induced transcription factor-1 α , NF- κ B, activator protein-1, etc. (9, 11, 28, 29), have been suggested as a probable mode of regulation of specific genes that may control cellular red ox status. Enhanced mitochondrial activity (13), suppression of glutathione *S*-transferase- π expression, and a reduction in the level of total glutathione specifically in CaP cells (8) have also been suggested as probable pathways for an increase in ROS production in CaP. A direct effect of androgen in regulating any of these pathways has yet to be shown. To the best of our knowledge, this is the first report of androgen-induced regulation of a rate-limiting enzyme of a specific biochemical pathway (polyamine catabolism) that is directly related to cellular oxidative stress induction. Because of the high levels of polyamines present in human prostate and CaP cells, this pathway seems all the more important in regulating oxidative stress in the prostate gland and specifically in CaP cells. The spermine level in LNCaP cells reported here is by far the highest among most of the cell lines reported thus far (ref. 31 and related references therein). A higher basal metabolism of spermine may be

one reason for the relatively higher ROS level in LNCaP cells compared with other cell lines (12).

A close inspection of the SSAT gene sequence reveals that there are four glucocorticoids response elements (GRE) but no androgen response element (ARE) upstream of the SSAT transcription start site. It has been reported that androgen receptor binds and activates GRE containing promoters (32). Its efficiency of activating promoters containing GRE, however, is much lower than that of activating promoters containing ARE. This may be one reason why the SSAT activation and the consequent ROS production was observed only when the cells were treated with high concentration (≥ 0.5 nmol/L) of R1881 but not with low concentration (≤ 0.05 nmol/L) of R1881 (ref. 12; Fig. 1).

Lastly, a decrease in cellular polyamine levels has been related to a delay in tumor growth and progression both in cell culture as well as in animals and humans (33–38). In this report, we observed a significant delay in tumor growth by CPC-200 (Fig. 5) although there is an increase, and not a decrease, in cellular spermidine and putrescine levels and no observable change in cellular spermine level. Therefore, change in cellular polyamine levels is probably not a cause for the delay in tumor progression in the TRAMP \times FVB animals developing spontaneous prostate tumor. The detail study of the polyamine and Ac-polyamine levels

in the TRAMP animal and tumor tissue has now been undertaken to confirm this point.

To the best of our knowledge, this is the first report of SSAT induction by a hormone (hormone analogue) R1881. Identification of androgen-induced polyamine catabolism leading to enhanced oxidative stress in the prostate cells and significant inhibition of CaP progression by blocking this pathway should open up a new avenue for CaP chemoprevention.

Disclosure of Potential Conflicts of Interest

H.S. Basu and G. Wilding: employment, ownership interest, and/or consultant/advisory board, Colby Pharmaceutical Company. The other authors disclosed no potential conflicts of interest.

Acknowledgments

Received 6/27/08; revised 6/17/09; accepted 7/2/09; published OnlineFirst 9/22/09.

Grant support: NIH, DOD, and Prostate Cancer Foundation.

The costs of publication of this article were defrayed in part by the payment of page charges. This article must therefore be hereby marked *advertisement* in accordance with 18 U.S.C. Section 1734 solely to indicate this fact.

We thank University of Wisconsin Paul P. Carbone Comprehensive Cancer Center Analytical Instrumentation Laboratory for Pharmacokinetics, Pharmacodynamics, and Pharmacogenetics for support in the acquisition of polyamine level determination using HPLC method.

References

1. Cerutti PA. Prooxidant states and tumor promotion. *Science* 1985;227:375–81.
2. Oberley TD, Oberley LW. Oxygen radicals and cancer. In: Yu BP, editor. *Free Radicals In Aging*. Ann Arbor (MI): CRC Press; 1993. p. 247–67.
3. Rautalahti M, Huttunen J. Antioxidants and carcinogenesis. *Annals Med* 1994;26:435–41.
4. Feig DI, Reid TM, Loeb LA. Reactive oxygen species in tumorigenesis. *Cancer Res* 1994;54:1890–4s.
5. Wilding G. Endocrine control of prostate cancer. *Cancer Surveys* 1995;23:43–62.
6. Dargel R. Lipid peroxidation—a common pathogenic mechanism? *Exp Toxic Pathol* 1992;44:169–81.
7. Sikka SC. Role of oxidative stress response elements and antioxidants in prostate cancer pathobiology and chemoprevention—a mechanistic approach. *Curr Med Chem* 2003;10:2679–92.
8. Lee WH, Morton RA, Epstein JD, et al. Cytidine methylation of regulatory sequences near the pi-class glutathione S-transferase gene accompanies human prostatic carcinogenesis. *Proc Natl Acad Sci U S A* 1994;91:11733–7.
9. Schulze-Osthoff K, Bauer M, Vogt M, Wesselborg S, Baeuerle PA. Reactive oxygen species as primary and second messengers in the activation of transcription factors. In: Forman HJ, Cadenas E, editors. *Oxidative Stress and Signal Transduction*. New York (NY): Chapman and Hall; 1997. p. 239–59.
10. Mehraein-Ghomi F, Lee E, Church DR, Thompson TA, Basu HS, Wilding G. JunD mediates androgen-induced oxidative stress in androgen dependent LNCaP human prostate cancer cells. *Prostate* 2008;68:924–34.
11. Church DR, Lee E, Thompson TA, Basu HS, Ripple MO, Ariazi EA, Wilding G. Induction of AP-1 activity by androgen activation of the androgen receptor in LNCaP human prostate carcinoma cells. *Prostate* 2005;63:155–68.
12. Ripple MO, Henry WF, Rago RP, Wilding G. Prooxidant-antioxidant shift induced by androgen treatment of human prostate carcinoma cells. *J Natl Cancer Inst* 1997;89:40–8.
13. Ripple MO, Hagopian K, Oberley TD, Schatten H, Weindruch R. Androgen-induced oxidative stress in human LNCaP prostate cancer cells is associated with multiple mitochondrial modifications. *Antioxid Redox Signal* 1999;1:71–81.
14. Ripple MO, Henry WF, Schwarze SR, Wilding G, Weindruch R. Effect of antioxidants on androgen-induced AP-1 and NF- κ B DNA-binding activity in prostate carcinoma cells. *J Natl Cancer Inst* 1999;91:1227–32.
15. Sun XY, Donald SP, Phang JM. Testosterone and prostate specific antigen stimulate generation of reactive oxygen species in prostate cancer cells. *Carcinogenesis* 2001;22:1775–80.
16. Oberley TD, Zhong W, Szweda LI, Oberley LW. Localization of antioxidant enzymes and oxidative damage products in normal and malignant prostate epithelium. *Prostate* 2000;44:144–55.
17. Tam NN, Nyska A, Maronpot RR, et al. Differential attenuation of oxidative/nitrosative injuries in early prostatic neoplastic lesions in TRAMP mice by dietary antioxidants. *Prostate* 2006;66:57–69.
18. Tam NN, Leav I, Ho SM. Sex hormones induce direct epithelial and inflammation-mediated oxidative/nitrosative stress that favors prostatic carcinogenesis in the noble rat. *Am J Pathol* 2007;171:1334–41.
19. Hatziaepostolou M, Polytaichou C, Katsoris P, Courty J, Papadimitriou E. Heparin affini regulatory peptide/pleiotrophin mediates fibroblast growth factor 2 stimulatory effects on human prostate cancer cells. *J Biol Chem* 2006;281:32217–26.
20. Cohen SS. In: *A Guide to the polyamines*. Oxford (UK): Oxford University Press; 1998. p. 296–319.
21. Casero RA, Jr., Wang Y, Stewart TM, et al. The role of polyamine catabolism in anti-tumour drug response. *Biochem Soc Trans* 2003;31:361–5.
22. Ha HC, Woster PM, Yager JD, Casero RA, Jr. The role of polyamine catabolism in polyamine analogue-induced programmed cell death. *Proc Natl Acad Sci U S A* 1997;94:11557–62.
23. Bey P, Bolkenius FN, Seiler N, Casara P. N-2,3-butadienyl-1,4-butanediamine derivatives: potent irreversible activators of mammalian polyamine oxidase. *J Med Chem* 1985;28:1–2.
24. Seiler N. Thirty years of polyamine-related approaches to cancer therapy. Retrospect and prospect: Part 2. Structural analogues and derivatives. *Curr Drug Targets* 2003;4: 565–85.
25. Xiao L, Celano P, Mank AR, et al. Structure of the human spermidine/spermine N1-acetyltransferase gene (exon/intron gene organization and localization to Xp22.1). *Biochem Biophys Res Commun* 1992;187:493–502.
26. Libby PR, Bergeron RJ, Porter CW. Structure-Function correlations of polyamine analog-induced increases in spermidine/spermine acetyltransferase activity. *Biochem Pharmacol* 1989;38:1435–42.
27. Kabra PM, Lee HK, Lubich WP, Marton LJ. Solid-phase extraction and determination of dansyl derivatives of unconjugated and acetylated polyamines by reversed-phase liquid chromatography: improved separation systems for polyamines in cerebrospinal fluid, urine and tissue. *J Chromatogr* 1986;380:19–32.
28. Greenberg NM, DeMayo F, Finegold MJ, et al. Prostate cancer in a transgenic mouse. *Proc Natl Acad Sci U S A* 1995;92:3439–43.
29. Kaplan-Lefko PJ, Chen T-M, Ittmann MM, et al. Pathobiology of autochthonous prostate cancer in a pre-clinical transgenic mouse model. *Prostate* 2003;55:219–37.
30. Gaboriau F, Vaultier M, Moulinoux JP, Delcros JG. Antioxidative properties of natural polyamines and dimethylsilane analogues. *Redox Rep* 2005;10:9–18.
31. Thomas T, Thomas TJ. Polyamine metabolism and cancer. *J Cell Mol Med* 2003;7:113–26.
32. De Vos P, Schmitt J, Verhoeven G, Stunnenberg HG. Human androgen receptor expressed in HeLa cells activates transcription *in vitro*. *Nucleic Acids Res* 1994;22:1161–6.
33. Frydman B, Blokhin AV, Brummel S, et al. Cyclopropane-containing polyamine analogues are efficient growth inhibitors of a human prostate tumor xenograft in nude mice. *J Med Chem* 2003;46:4586–600.
34. Basu HS, Pellarin M, Feuerstein BG, et al. Interaction of a polyamine analogue, 1,19-bis-(ethylamino)-5,10,15-triazanonadecane (BE-4-4-4-4), with DNA and effect on growth, survival, and polyamine levels in seven human brain tumor cell lines. *Cancer Res* 1993;53:3948–55.
35. Hu RH, Pegg AE. Rapid induction of apoptosis by deregulated uptake of polyamine analogues. *Biochem J* 1997;328:307–16.
36. Kee K, Vujcic S, Merali S, et al. Metabolic and antiproliferative consequences of activated polyamine catabolism in LNCaP prostate carcinoma cells. *J Biol Chem* 2004;279:27050–8.
37. Frydman B, Porter CW, Maxuitenko Y, et al. A novel polyamine analog (SL-11093) inhibits growth of human prostate tumor xenografts in nude mice. *Cancer Chemother Pharmacol* 2003;51:488–92.
38. Hahm HA, Ettinger DS, Bowling K, et al. Phase I study of N(1),N(11)-diethylnorspermine in patients with non-small cell lung cancer. *Clin Cancer Res* 2002;8:684–90.